

# Anaerobic Co-Digestion of Products from Biosolids Pyrolysis – Implementation in ADM1

Gudny Øyre Flatabo<sup>a,b,\*</sup>, Wenche Hennie Bergland<sup>a</sup>

<sup>a</sup> Department of Process, Energy and Environmental Technology, University of South-Eastern Norway, Kjølnes ring 56, 3918 Porsgrunn, Norway, <sup>b</sup> Scanship AS, Nedre Langgate 19, 3126 Tønsberg, Norway.  
gudny.flatabo@scanship.no

## Abstract

Pyrolyzing biosolids can decrease volume and increase value of solids while anaerobic digestion of gas and liquids from the process could increase overall methane production. Prediction of process behavior and biogas yield through simulation is valuable when considering new substrates for anaerobic digestion. In this study, gas and liquids from biosolids pyrolysis were implemented in Anaerobic Digestion Model No 1 (ADM1) together with a stream of thermally hydrolyzed sludge/food waste used in an industrial biogas plant. Average operational data from the industrial plant was used to calibrate the base scenario in ADM1, achieving a good fit. Simulation scenarios evaluating two hydrolysis constants for the pyrolysis liquid showed minor differences at the load simulated and simulated variations in composition of the liquid showed minor differences. Simulation of adding a relevant stream of pyrolysis liquid and gas together increased methane production by 7 % but decreased overall methane yield from 63 % to 61 % compared to the base scenario.

## 1. Introduction

Pyrolysis is a thermochemical process that converts dry biomass into gas, solids, and liquids at high temperatures without oxygen. The process can yield value added products such as biochar, pyrolysis gas, and condensable liquids. Biochar offers carbon and nutrient capture (Lehmann *et al.*, 2021) and pyrolysis gas and condensable liquids are energy carriers or chemicals precursors (Jahangiri *et al.*, 2021). Anaerobic digestion (AD) is a biochemical process where microorganisms decompose wet biomass in the absence of oxygen, to simple chemicals such as acetate, H<sub>2</sub>, and CO<sub>2</sub>. These simple chemicals are then converted to methane by methanogens. The resulting mix of methane and CO<sub>2</sub> is called biogas. The residual biomass, digestate, is normally dewatered to reduce volume and is then called biosolids. Biogas can be used to produce heat and electricity or be upgraded to biomethane for use as a fuel similar to fossil (“natural”) gas. Biosolids can normally be applied to land as a fertilizer, but if sewage sludge is the source, there are many limitations to its use making its disposal a large cost for AD plants.

Pyrolysis gas contains varying amounts of H<sub>2</sub>, CO<sub>2</sub>, CO, CH<sub>4</sub>, and other C<sub>2+</sub> gases, and has been successfully converted to biogas via anaerobic digestion (Luo and Angelidaki, 2012; Luo *et al.*, 2013; Li *et al.*, 2020; Torri *et al.*, 2020). AD of pyrolysis liquids from various feedstocks has also been studied (Seyedi *et al.*, 2020; Ghimire *et al.*, 2021). Successful co-digestion of liquid and gaseous pyrolysis products in an industrial process might

increase biogas production from initial feedstock, but it might also upset process behavior. Prediction through simulation is valuable when considering new AD substrates or new process conditions. The Anaerobic digestion model No. 1 (ADM1) was developed by the International Water Association to predict AD process behavior by many substrates and conditions (Batstone *et al.*, 2002). However, simulations using the standard ADM1 cannot predict process behavior for AD of unusual substrates such as pyrolysis gas and liquids and needs modification when implementing such substrates.

Currently, some works have focused on implementing mixtures of CO, H<sub>2</sub>, and CO<sub>2</sub> (syngas) into ADM1, providing explanations of the model and necessary extensions (Shah *et al.*, 2017; Sun *et al.*, 2021). Simulation of combined pyrolysis liquid and gas has not been explored in the literature, and in the few experimental works on AD of real pyrolysis gas, it has been cleaned and condensed first (Giwa *et al.*, 2019; Torri *et al.*, 2020). The authors have argued that the liquid may be inhibitory and have either disposed of or digested it in a separate reactor from the gas. Possible inhibition from pyrolysis liquid from lignocellulosic materials implemented in ADM1 was presented at EUROSIMS 2021 (Raya *et al.*, 2021), while Seyedi (2020) experimented with several methods to decrease AD toxicity from biosolids pyrolysis liquid. Results from Seyedi (2020) were not implemented in any AD model, but the data showed most success in reducing toxicity from biosolids pyrolysis liquid when using acclimated inoculum

and a low loading rate (0.03 gCOD L<sup>-1</sup>d<sup>-1</sup>) with correspondingly long solids retention time.

Pyrolysis liquid from biosolids have different properties compared to liquid from lignocellulosic materials, such as much higher total ammonia nitrogen (TAN) content (Seyedi *et al.*, 2019). In ADM1, inhibition from NH<sub>3</sub> on acetate degrading organisms is modelled using a non-competitive reversible inhibition term (Eq. 1) (Batstone *et al.*, 2002).

$$I = \frac{1}{1 + S_1/K_1} \quad (1)$$

Where the total inhibition, *I*, is calculated using the inhibitor concentration *S*<sub>1</sub> (NH<sub>3</sub>, M) and the inhibition parameter *K*<sub>1</sub>, set to 0.0018 M as the inhibitory free ammonia concentration. The higher the inhibitor concentration *S*<sub>1</sub> goes, the lower the total inhibition value, *I*, gets, corresponding to more inhibition. A lower loading rate, such as suggested by Seyedi (2020) would reduce inhibitor concentration and reduce total inhibition (increase *I*). Simulations of co-digestion with high TAN pyrolysis liquid in an industrial process can give indications of tolerance limits for the microbial processes. Simulating at industrially relevant loading rates and co-digestion ratios gives rapid results on whether the process and loading are hypothetically viable in an industrial setting.

### 1.1. Goal and scope

Through this study, we aim to implement gas and liquid from biosolids pyrolysis in ADM1 and simulate anaerobic co-digestion of pyrolysis products using industrially relevant ratios of pyrolysis products to main substrate.

The study includes the following: a base scenario simulating and calibrating an industrial AD process using operational and laboratory data, an implementation of pyrolysis liquid using a combination of laboratory and literature based compositional data, an evaluation of hydrolysis constant for the implemented pyrolysis liquid, a comparison of effect of pyrolysis liquid composition on simulation results, and a combination scenario including pyrolysis liquid and gas.

We do not address additional inhibition from pyrolysis liquid products, as we hypothesize that our loading rate is sufficiently low and diluted by the main substrate, and that the high total ammonium nitrogen concentration will make inhibition by ammonia more important than other potential inhibitors.

## 2. Methodology

Samples of the main substrate, hydrolyzed sludge (HS), digestate, and pyrolysis products were collected and analyzed for relevant compositional data to implement in ADM1. ADM1 extended with syngas addition from Shah *et al.* (2017) was used as

a basis and extended with an extra product stream of pyrolysis liquid with separate hydrolysis constant.

### 2.1. Materials

Main substrate and digestate was sampled from a mesophilic sewage sludge/food waste continuously fed stirred tank (CSTR) industrial AD plant. At this plant, a thermal hydrolysis process (THP) at 160°C is used to pre-treat and sterilize the substrate. HS for analysis was sampled after the THP, prior to entering the AD bioreactors.

Pyrolysis liquid was provided by Scanship AS and produced from pyrolysis at 600°C of dried and pelletized biosolids from AD at the same plant, using the Biogreen® technology. Pyrolysis gas was condensed down to 5-8°C and the condensate, pyrolysis liquid (PL), was collected. The PL was a heterogeneous liquid: an emulsion of unevenly distributed organic phases in an aqueous phase. It was not possible to separate the liquid into an organic and an aqueous phase by gravity.

### 2.2. Analytical methods

Main substrate and digestate was analyzed for Chemical Oxygen Demand (total and soluble: tCOD and sCOD), total ammonium nitrogen (TAN), pH and volatile fatty acids (VFAs: acetic acid, propionic acid, butyric acid, iso-butyric acid, valeric acid, iso-valeric acid, caprioic acid, iso-caprioic acid and heptanoic acid), previously described (Bergland *et al.* 2015).

Dried samples of substrate and digestate were analysed for Total Kjeldahl Nitrogen (TKN) to estimate protein content, crude fat (EC, 2009) to estimate lipids content, and water soluble carbohydrates (Randby *et al.*, 2010) to estimate sugars.

Pyrolysis liquid was analysed for TAN, pH, VFAs, and total acid capacity (Supelco test kit no. 101758, for an indication of inorganic carbon) in addition to elemental analysis (ASTM D1552-16, 2021; ASTM D5291-21, 2021).

Pyrolysis gas was sampled in a gas bag during pyrolysis and composition was analysed using gas chromatography with two detectors: Pulsed Discharge Helium Ionisation Detector (PDHID, VIDI) and Thermal Conductivity Detector (TCD, Agilent). Helium was used as carrier gas and two different columns were used (Restek MXT Molsieve 5Å, 30 m, and Varian Poraplot Q, 25 m).

### 2.3. Modelling and Simulation

A full-scale AD bioreactor was simulated (base scenario) using ADM1 in AquaSim Version 2.1f. Relevant biogas production data was obtained from biogas plant operators and used as input data for the model. Known compositional data from the pyrolysis products PL and pyrolysis gas was then added, using relevant pyrolysis yields obtained from

pyrolysis operators. Simulation of PL evaluates hydrolysis rate and PL composition. Simulation of pyrolysis gas addition does not include the process of diffusion solubilizing the gas into the bioreactor volume and assumes the whole syngas volume flow is available for the microorganisms. Operational data to compare with simulation results was only available for the base scenario.

### 2.3.1. Base scenario

The base scenario was calibrated against average operational data (Tab. 1) from an ongoing industrial biogas plant running on thermally hydrolyzed sludge/food waste.

Table 1: Average production data from industrial AD plant, used for calibrating the base scenario. HS = hydrolyzed sludge, HRT = hydraulic retention time.

Production data	Unit	Average value
HS <sub>load</sub>	m <sup>3</sup> d <sup>-1</sup>	183
Volume <sub>bioreactor</sub>	m <sup>3</sup>	3500
HRT	d	19.1
Production <sub>biogas</sub>	Nm <sup>3</sup> d <sup>-1</sup>	8374
%vol CH <sub>4</sub>	%vol	63.0
tCOD <sub>digestate</sub>	kg m <sup>-3</sup>	54.0
sCOD <sub>digestate</sub>	kg m <sup>-3</sup>	5.30
pH <sub>digestate</sub>		7.87
TAN <sub>digestate</sub>	kmol N m <sup>-3</sup>	0.104

Compositional results of the dry substrate for protein, lipids and sugar were adjusted to 9 % Total Solids (TS, typical value for the AD plant), while measured VFAs were input additionally, assuming these had been lost during drying while measuring TS. Complex VFAs (caproic acid, iso-caproic acid and heptanoic acid), not included in the model, were input as sugars. Amount of inerts were estimated from operational data. Lipids were estimated based on crude fat results, while proteins were estimated based on TKN results after subtracting TAN values. Carbohydrates were estimated as the difference needed to make up measured tCOD. Tab. 2 lists the inputs used for the simulation.

Table 2: Input compositional concentrations for base scenario. COD values add up to a total COD of 130 kg m<sup>-3</sup>. Soluble input values for amino acids, inerts, and long chain fatty acids are not listed.

Input data	Unit	Value
Lipids	kg COD m <sup>-3</sup>	36.7
Carbohydrates	kg COD m <sup>-3</sup>	53.4
Protein	kg COD m <sup>-3</sup>	11.7
Sugar	kg COD m <sup>-3</sup>	0.223
Acetic acid	kg COD m <sup>-3</sup>	1.84
Propionic acid	kg COD m <sup>-3</sup>	0.686
Butyric acid	kg COD m <sup>-3</sup>	0.806
Valeric acid	kg COD m <sup>-3</sup>	0.491
Total inert	kg COD m <sup>-3</sup>	23.4
Inorganic nitrogen	kmol N m <sup>-3</sup>	0.0976
Inorganic carbon	kmol HCO <sub>3</sub> <sup>-</sup> m <sup>-3</sup>	0.0800

Measured total COD at 9 % TS was 130 kg m<sup>-3</sup>, while soluble COD was 21.8 kg m<sup>-3</sup>. Soluble amino acids were set to 7.2 % of protein COD, as the average solubilization from two sludges treated with thermal hydrolysis in Chen *et al.* (2019). Soluble inerts were set to 8.9 % of inerts based on operational data. Soluble long chain fatty acids were used to make up measured sCOD difference. Inorganic carbon is not known but is assumed based on biogas composition operational data (63% methane, Tab. 1). Additional ions may be present, used in pH simulation, requiring adjustment of the ion balance. The base scenario has a relatively high pH (7.87, Tab. 1), so an adjustment term was added to the cations (0.35 M) to reach the target.

### 2.3.2. Pyrolysis liquid input

Due to the emulsified nature of the PL, only water-soluble COD could be tested with good accuracy. Because of this, the total COD of PL was represented by theoretical oxygen demand, calculated based on elemental composition (OECD, 1992).

PL was added to ADM1 as an additional substrate load, without changing volume load from HS or total volume of reactor, thus reducing the overall hydraulic retention time (HRT).

The PL load (Tab. 3) was based on the pyrolysis mass yield when pyrolyzing biosolids from the same AD process, assuming all PL goes back into the process. Fig. 1 outlines the mass load estimation for PL and pyrolysis gas. In our case, residual mass in digestate is dewatered and dried to 86 % TS, pyrolyzed, yielding 50 % mass pyrolysis gases and liquids, divided between 33 % mass liquids (4 t) and 17 % mass gases (2 t).

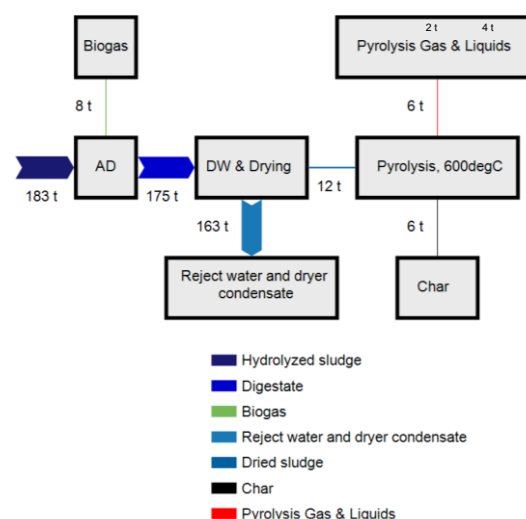


Figure 1: Simplified mass balance of industrial anaerobic digestion (AD) with pyrolysis of biosolids. DW = dewatering.

The biomethane potential (BMP) of the PL is unknown, and to simulate PL digestion the amount

of inert must be estimated. Seyedi *et al.* (2019) tested the BMP of pyrolysis liquid produced from biosolids, spiked with acetate. They found that methane production was highly affected by the organic load of PL. To estimate the concentration of inerts in our PL, a linear curve was fitted to methane % yield data estimated from the three lowest COD loadings from Seyedi *et al.* (2019) adjusted for the control (Fig. 2). The two lowest loadings gave relatively high methane yield (%), while the third lowest, 0.6 g COD L<sup>-1</sup>, resulted in less methane production than the control and was adjusted to 0 when fitting a linear model. The linear model gave a methane yield of 40 % based on our calculated loading of 0.41 g COD L<sup>-1</sup> (Fig. 2, X), corresponding to 60 % inert.

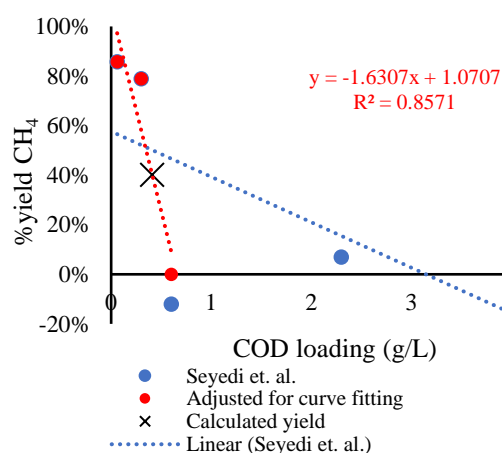


Figure 2: Methane yield of pyrolysis liquid from biosolids pyrolysis based on COD loading. Adjusted for control sample, based on data from (Seyedi *et al.*, 2019). Blue dots show all COD loadings tested by Seyedi *et al.* (2019), some have a negative yield because they produced less than the control sample. Red dots show the two loadings with a positive yield and the first negative yield adjusted to 0. The black X shows the calculated value for our data.

Compositional data was not available for PL, but analyses of the digestate gave an indication of protein and lipid content going into the pyrolysis. As a simplification and approximation of PL composition, the mass yield of compounds relevant for AD (Tab. 4) were used to adjust the protein and

lipid content in the digestate to input values for protein and lipids from PL (Wang *et al.*, 2017).

To account for the uncertainties concerning the composition of PL, an additional three compositional variations were simulated (Tab. 5). For all scenarios PL inorganic nitrogen and inorganic carbon was set to the measured TAN and total acid capacity values, 1.085 mol/L for IN and 0.700 mol/L for IC. Soluble inerts were used to add up the sCOD and are added together with particulate inerts in Tab. 5.

Table 3: Load data when adding pyrolysis liquid (PL) to the base scenario. HRT = hydraulic retention time.

Production data	Unit	Value
PL <sub>load</sub>	m <sup>3</sup> d <sup>-1</sup>	4.08
Total load <sub>(HS+PL)</sub>	m <sup>3</sup> d <sup>-1</sup>	187
Volume <sub>bioreactor</sub>	m <sup>3</sup>	3500
HRT	d	18.7
tCOD <sub>PL</sub>	kg m <sup>-3</sup>	352
sCOD <sub>PL</sub>	kg m <sup>-3</sup>	194
Load <sub>tCOD_PL</sub>	kg d <sup>-1</sup>	1440
Load <sub>tCOD_(HS+PL)</sub>	kg d <sup>-1</sup>	25200
HS <sub>loading rate</sub>	kg COD m <sup>-3</sup> d <sup>-1</sup>	6.80
PL <sub>loading rate</sub>	kg COD m <sup>-3</sup> d <sup>-1</sup>	0.410
(HS+PL) <sub>loading rate</sub>	kg COD m <sup>-3</sup> d <sup>-1</sup>	7.21

Table 4: Mass yields (%) of relevant compounds for AD, from liquid from pyrolysis of proteins and lipids extracted from a microalga. From Wang *et al.* (2017).

Compounds type	Protein	Lipid
Amines and Amides (<C8)	1.94	0.43
Carboxylic acids	0.45	44.46
Ketones and Aldehydes (<C8)	4.82	0.53
Alcohols (<C8)	0	2.23
Alcohols (>C8)	0	0.36
Phenols	2.87	0
Esters	8.19	15.25
Ethers	1.92	0.12
Total	20.19	63.38

### 2.3.3. Hydrolysis constants

In the original ADM1, Batstone *et al.* (2002) used a complex particulates variable as a general variable for particulates in a substrate.

Table 5: Input compositional data for four scenarios with additional pyrolysis liquid. All units are concentration, kg COD m<sup>-3</sup>. COD values add up to a total COD of 352 kg m<sup>-3</sup>.

Input data	PL <sub>most relevant</sub>	PL <sub>lipids=carbs</sub>	PL <sub>low protein</sub>	PL <sub>high protein</sub>
Lipids	37.4	23.5	41.2	21.6
Carbohydrates	9.53	23.5	9.53	9.53
Protein	7.66	7.66	3.83	23.5
Sugar	18.1	18.1	18.1	18.1
Acetic acid	40.6	40.6	40.6	40.6
Propionic acid	9.45	9.45	9.45	9.45
Butyric acid	10.3	10.3	10.3	10.3
Valeric acid	8.23	8.23	8.23	8.23
Inert	111	111	111	111

A disintegration process was the rate limiting step for this variable. The variable was especially designed for complex sludge such as waste activated sludge and for microbial biomass and uses a disintegration constant of 0.5 d<sup>-1</sup> as standard. However, this input decomposes into 30 % each of lipids, carbohydrates, protein and 10 % inert. Our substrates have more accurate compositional data to input directly, making the hydrolysis process the rate limiting step. The standard hydrolysis constant,  $k_{hyd}$ , in the original ADM1 is 10 d<sup>-1</sup>, which is a very high value meaning that the hydrolysis step goes very quickly and is not rate limiting.

Koch and Drewes (2014) compared two common methods of fitting biomethane potential (BMP)-curves to estimate the hydrolysis constant and derived an alternative approach where the only input necessary is the time,  $t$ , it takes for the daily methane production to drop to <1 % of accumulated value, and keep this low production for at least three days, according to the German Guideline VDI 4630 (VDI 4630, 2016). The alternative calculation of  $k_{hyd}$  based on BMP-time,  $t$ , is shown as Eq. 2 below:

$$k_{hyd} = \frac{t - 100}{t - t^2} \quad (2)$$

Raya (2021) tested a sample of the main substrate inoculated with its digestate and got a clear end of the experiment by day 10. Substituting  $t$  with days gives  $k_{hyd} = 1$  d<sup>-1</sup> for the main substrate, double of the original disintegration constant. This seems like a probable value for thermally hydrolyzed sludge, which normally is digested faster than untreated sludge.

When evaluating hydrolysis constant for the pyrolysis liquid (PL), the data, however, is not clear. The BMP tests performed by Seyedi *et al.* (2019) drops to <1 % daily production after 17 days, but the production goes higher again some days later, the latest being 30 days when no daily production higher than 1% is seen. This corresponds to  $k_{hyd}$  values of 0.3 (17 days) and 0.08 (30 days). To evaluate the effect of the different  $k_{hyd}$  values, both were tested using the most relevant PL composition (Tab. 5).

### 2.3.4 Gas addition

Evaluating the gas effect on the processes occurring in AD is done by simplification where technical dissolution challenges are assumed solved by ignoring physical barriers and adding the gas as an extra source of COD without increasing the total liquid substrate volume stream (Shah *et al.*, 2017). This has been achieved in laboratory experiments (Corbellini *et al.*, 2021) where hydrogen gas has been injected at similar organic loading rate below surface level and with high mixing speed, achieving 90-99 % conversion efficiency, which might improve with further acclimation. Since hydrogen gas is the least soluble in water, we assume carbon monoxide can be transferred with similar efficiency

(solubility H<sub>2</sub> at 38°C: 0.0014 g gas/kg water, solubility CO at 38°C: 0.021 g gas/kg water, (Engineering ToolBox, 2008)).

Table 6: Load of non-condensable gases, based on composition of gas measured during pyrolysis.

Gas loaded	Unit	Value
CO	kg COD d <sup>-1</sup>	182
H <sub>2</sub>	kg COD d <sup>-1</sup>	434
CH <sub>4</sub>	kg COD d <sup>-1</sup>	600
COD <sub>gas loading rate</sub>	kg COD m <sup>-3</sup> d <sup>-1</sup>	0.347
COD <sub>HS+PL+Gas loading rate</sub>	kg COD m <sup>-3</sup> d <sup>-1</sup>	7.56
CO <sub>2</sub>	kmol d <sup>-1</sup>	32.8
CO <sub>2</sub> input conc. in HS+PL vol	kmol m <sup>-3</sup> d <sup>-1</sup>	0.170

## 3. Results

### 3.1 Base scenario

The simulation results had a good fit with AD operational data and were within 1 % deviation (Tab. 7) except for total VFA.

Table 7: Measured and simulated values for the base scenario. Value units are kg COD m<sup>-3</sup> for all unlabeled except for gas production (m<sup>3</sup>), Total Ammonium Nitrogen (TAN, M d<sup>-1</sup>), and pH.

Target data	Value <sub>meas</sub>	Value <sub>sim</sub>	%Diff
Production <sub>biogas</sub>	8374	8409	0.418
Production <sub>CH<sub>4</sub></sub>	5275	5278	0.0569
% vol CH <sub>4</sub>	63.0	62.8	-0.317
tCOD <sub>digestate</sub>	54.0	54.0	0.000
sCOD <sub>digestate</sub>	5.30	5.33	0.566
pH <sub>digestate</sub>	7.87	7.83	-0.508
TAN <sub>digestate</sub>	0.104	0.103	-0.962
totVFA <sub>digestate</sub>	0.172	3.22	1782

### 3.2 Variation of hydrolysis constant

The simulation results of two scenarios with PL added with two different  $k_{hyd}$ , 0.3 d<sup>-1</sup> and 0.08 d<sup>-1</sup>, had very small differences, less than 0.6 % for all parameters. The main effect from the reduction of  $k_{hyd}$  was a higher tCOD concentration in the digestate (+0.4 %), a small decrease in biomass and biomass growth rates, and a minor decrease in biogas production (-0.3 %).

Due to the low difference between the simulation results using different hydrolysis constants, the higher and most likely value (0.3 d<sup>-1</sup>) was used for further simulations on composition and gas addition.

### 3.3 PL composition

#### 3.3.1 Lipids and carbohydrates

To see the impact on simulation from lipid and carbohydrate distribution in PL, lipids concentration was reduced, and carbohydrate concentration was increased to a scenario where these would contribute equal amounts of COD. This scenario was compared to the most relevant compositional distribution (Tab. 5). All the differences in simulation results at stable conditions were less than 1 %, except for simulated

total VFA in digestate, which was reduced by 1.15 % compared to the most relevant scenario.

### 3.3.2 Changing PL protein input

Higher protein content changed the simulation results to a much larger extent than the other compositional changes. The parameters most affected by the changes (Fig. 3) were: Acetic acid (9% increase), sCOD (4% increase), amino acid degrading organisms' biomass and growth rate (3% increase), TAN (2% increase) and inorganic carbon (1% decrease). The low protein content scenario decreased acetic acid and sCOD by 2 and 1 %, respectively, and otherwise showed small changes (Fig. 3).

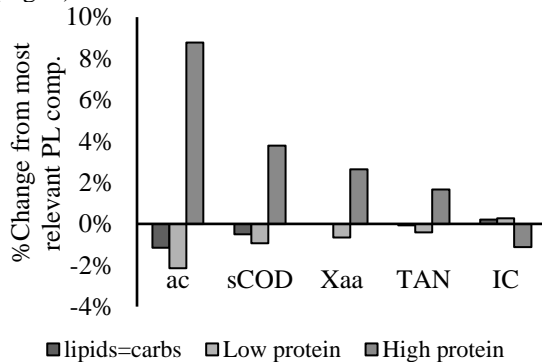


Figure 3: The parameters with the largest % change when comparing the three different composition scenarios to the most relevant composition (Tab. 5). ac = acetic acid left in digestate, sCOD = soluble chemical oxygen demand left in the digestate, Xaa = amino acid degrading organisms and their growth rate, TAN = total ammonium nitrogen left in digestate, IC = inorganic carbon in digestate.

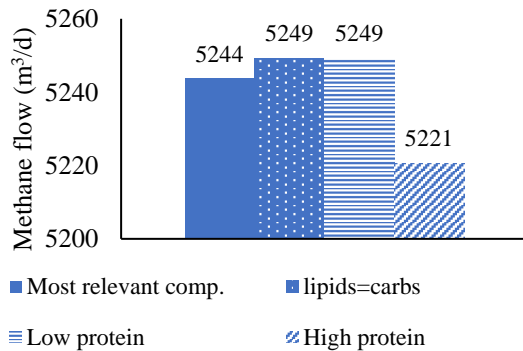


Figure 4: Daily simulated methane production when different PL input compositions are tested.

Simulated methane production only changed 0.1-0.5% by changing the protein load to the concentrations used in these scenarios (Tab. 5), but when comparing the results scaled (Fig. 4), it looks like a small trend where higher protein content affect methane production negatively. Like for the methane production, inhibition from  $\text{NH}_3$  increases slightly (lower inhibition value) with higher protein input (Fig. 5).

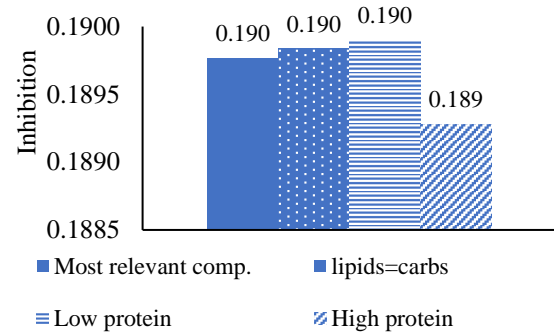


Figure 5: Inhibition values from ammonia ( $\text{NH}_3$ ) on acetoclastic methanogens and the difference between simulated PL compositions. Lower inhibition value means more inhibition.

### 3.4 Simulation of gas addition

Gas addition increased the simulated methane production with 7 %,  $375 \text{ Nm}^3 \text{ d}^{-1}$  more than the simulated base scenario (Fig. 6 and 9). The pyrolysis gas contained  $210 \text{ Nm}^3$  of  $\text{CH}_4$ , which accounts for about 56% of the increase in methane production. Inhibition from ammonia that increased (lower inhibition value) with PL addition, normalized somewhat when gas was added (from 0.19 with PL to 0.196 with PL and gas, Fig. 7).

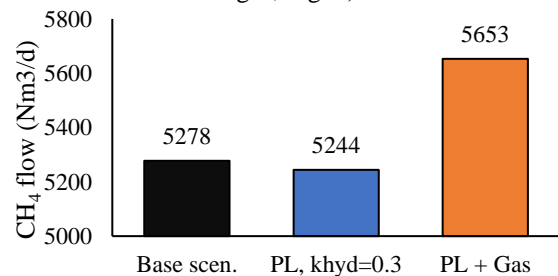


Figure 6: Daily simulated methane production for base scenario, added pyrolysis liquid and liquid and gas added together.

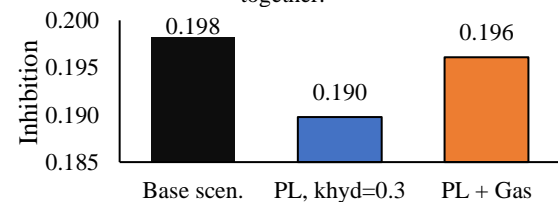


Figure 7: Inhibition values from  $\text{NH}_3$  on acetoclastic methanogens for base scenario, added pyrolysis liquid and liquid and gas added together. Lower inhibition value means more inhibition.

The largest change from the base scenario was the acetic acid concentration in digestate that nearly tripled (from  $1.6 \text{ kg COD m}^{-3}$  in base scenario to  $4.5 \text{ kg COD m}^{-3}$ , Fig. 8) when adding PL alone. The largest change for the gas scenario was the residual sCOD in the digestate, which increased by 55 % from the base scenario (Fig. 8). Biogas also had a significant increase of 14 % for the PL+Gas scenario (Fig. 9). TAN increased by about 20 % for both the scenarios (Fig. 8).

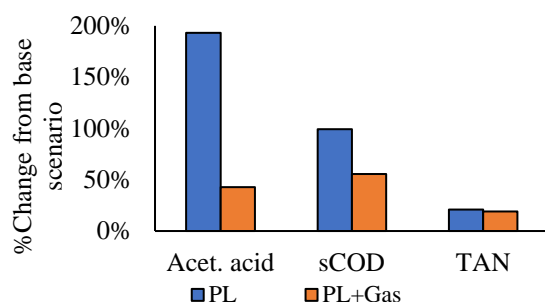


Figure 8: Percentage change from base scenario on acetic acid, soluble COD (sCOD) and TAN (total ammonium nitrogen) when adding pyrolysis liquid (PL) or pyrolysis liquid and gas (PL+Gas).

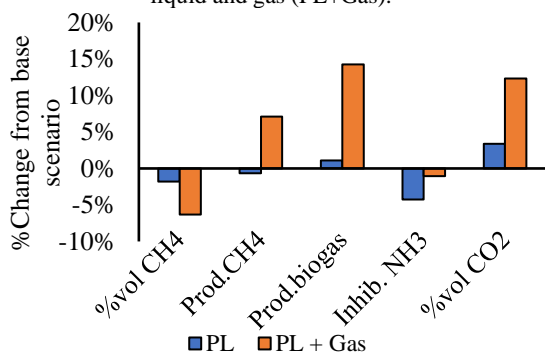


Figure 9: Percentage change from base scenario on methane concentration (% vol CH<sub>4</sub>), produced methane, produced biogas, ammonia inhibition (Inhib. NH<sub>3</sub>) and CO<sub>2</sub> concentration (% vol CO<sub>2</sub>) when adding pyrolysis liquid (PL) or pyrolysis liquid and gas (PL+Gas).

## 4. Discussions and Summary

### 4.1 Base scenario

The simulated base scenario was well calibrated to match operational and measured data for the industrial process, except for VFAs (Tab. 8), these are previously reported with low fit for thermally hydrolyzed sludge in ADM1 (Donoso-Bravo *et al.*, 2020).

### 4.2 Variations of PL hydrolysis and composition

Despite reducing the hydrolysis constant for the added PL to a fourth of the most relevant value, from 0.3 d<sup>-1</sup> to 0.08 d<sup>-1</sup>, the differences in the simulation results after stabilization were small at the simulated PL load. Reductions in biomass growth rates and increase in residual tCOD (section 3.3) are expected with slower solubilization of particulates caused by reducing the hydrolysis constant without changing the HRT. The % difference in biogas production, however, was less than the % difference between the simulated base scenario and measured operational data, so they would most likely not be noticed in an experimental or industrial setting.

Changing the simulated protein input had more effect than changing lipid and carbohydrate distribution. More protein leads to higher TAN (0.127 M for the high protein scenario, up from 0.125 M for the most relevant scenario), which

increases inhibition by ammonia of acetoclastic methanogenesis (Fig. 5) causing a higher concentration of acetic acid in the digestate (Fig. 3, 8 % increase in this scenario) and lower overall methane production (Fig. 4). In our scenario, the process is still stable as the pH has not decreased by much, but it gives a clear indication of what happens with too much loaded protein.

Most likely, however, the PL does not contain “traditional” lipids, carbohydrates and protein, as these are decomposed and changed into other compound groups through pyrolysis (e.g. Tab. 4 and Wang *et al.* (2017)). PL from biosolids does contain a lot of nitrogen, however. From our total nitrogen analysis there is still 1.4 M nitrogen bound to unknown compounds, after correcting for ammonium-N. Whether these compounds are anaerobically digested with an effect like proteins, whether they stay inert or whether they are inhibitory to the process is difficult to predict without conducting carefully planned, long-term continuous experiments.

### 4.3 Effects on industrial process from pyrolysis liquid and gas

The simulated methane production drops slightly when adding PL alone but increases 7 % when gas is added. From the overview figures (Fig. 8 and 9) we see that acetic acid concentration triples when PL is added, and TAN concentration increases, causing more inhibition from ammonia on acetoclastic methanogens. This might explain why the methane production drops slightly despite the PL contributing extra COD to the process (0.4 kg COD m<sup>-3</sup> d<sup>-1</sup>, Tab. 3).

The overall methane yield drops compared to the base scenario when adding these pyrolysis products (Fig. 10), most likely due to the high load of inorganic nitrogen in the liquid fraction.

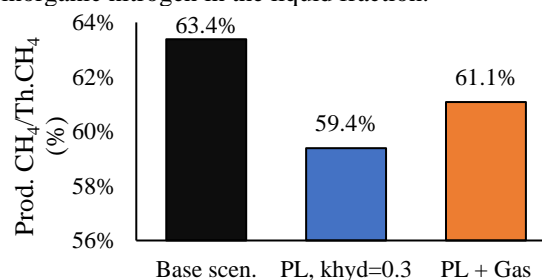


Figure 10: %Methane yields for the overall processes.

In combination, the slightly inhibitory effect from the PL is “diluted” by the gas, so the actual methane production still increases overall, however with less overall efficiency compared to the extra added COD. Despite the possible problems with PL in AD, the result from the combined addition indicates that the processes occurring in AD may tolerate an uncondensed pyrolysis gas co-substrate and increase methane production moderately.

## Acknowledgment

The authors would like to thank and acknowledge master student Nasim Mohajeri Nav who has performed and participated extensively in the lab work for this study. The study was funded by the Norwegian Research Council and Scanship AS through the Industrial PhD-program.

## References

- ASTM D1552-16 (2021) 'Standard Test Method for Sulfur in Petroleum Products by High Temperature Combustion and Infrared (IR) Detection or Thermal Conductivity Detection (TCD)', in Subcommittee 03 (ed.) *Book of Standards*. ASTM International, pp. 1–5. Available at: <https://www.astm.org/d1552-16r21.html> (Accessed: 23 May 2022).
- ASTM D5291-21 (2021) 'Standard Test Methods for Instrumental Determination of Carbon, Hydrogen, and Nitrogen in Petroleum Products and Lubricants', in Subcommittee 03 (ed.) *Book of Standards*. ASTM International, pp. 1–8. doi: 10.1520/D5291-21.
- Batstone, D. J. *et al.* (2002) 'The IWA Anaerobic Digestion Model No 1 (ADM1)', *Water Science and Technology*. IWA Publishing, 45(10), pp. 65–73. doi: 10.2166/WST.2002.0292.
- Bergland, W. H. *et al.* (2015) 'High rate manure supernatant digestion', *Water Research*. Elsevier Ltd, 76, pp. 1–9. doi: 10.1016/j.watres.2015.02.051.
- Chen, S. *et al.* (2019) 'Effects of thermal hydrolysis on the metabolism of amino acids in sewage sludge in anaerobic digestion', *Waste Management*. Pergamon, 88, pp. 309–318. doi: 10.1016/J.WASMAN.2019.03.060.
- Corbellini, V. *et al.* (2021) 'Performance Analysis and Microbial Community Evolution of in Situ Biological Biogas Upgrading with Increasing H<sub>2</sub>/CO<sub>2</sub>Ratio', *Archaea*. Hindawi Limited, 2021, pp. 1–15. doi: 10.1155/2021/8894455.
- Donoso-Bravo, A. *et al.* (2020) 'Exploitation of the ADM1 in a XXI century wastewater resource recovery facility (WRRF): The case of codigestion and thermal hydrolysis', *Water Research*. Pergamon, 175, p. 115654. doi: 10.1016/J.WATRES.2020.115654.
- EC, T. C. of the E. C. (2009) 'COMMISSION REGULATION (EC) No 152/2009 of 27 January 2009 laying down the methods of sampling and analysis for the official control of feed', *Official Journal of the European Union*, 54, p. 37.
- Engineering ToolBox (2008) *Solubility of Gases in Water vs. Temperature*. Available at: [https://www.engineeringtoolbox.com/gases-solubility-water-d\\_1148.html](https://www.engineeringtoolbox.com/gases-solubility-water-d_1148.html) (Accessed: 26 August 2022).
- Ghimire, N., Bakke, R. and Bergland, W. H. (2021) 'Liquefaction of lignocellulosic biomass for methane production: A review', *Bioresour. Technol.* Elsevier, 332, p. 125068. Available at: <https://linkinghub.elsevier.com/retrieve/pii/S0960852421004077> (Accessed: 8 April 2021).
- Giwa, A. S. *et al.* (2019) 'Pyrolysis of difficult biodegradable fractions and the real syngas bio-methanation performance', *Journal of Cleaner Production*. Elsevier Ltd, 233, pp. 711–719. doi: 10.1016/j.jclepro.2019.06.145.
- Jahangiri, H. *et al.* (2021) 'Thermochemical Conversion of Biomass and Upgrading of Bio-Products to Produce Fuels and Chemicals', *Catalysis for Clean Energy and Environmental Sustainability*. Springer, Cham, pp. 1–47. doi: 10.1007/978-3-030-65017-9\_1.
- Koch, K. and Drewes, J. E. (2014) 'Alternative approach to estimate the hydrolysis rate constant of particulate material from batch data', *Applied Energy*. Elsevier, 120, pp. 11–15. doi: 10.1016/J.APENERGY.2014.01.050.
- Lehmann, J. *et al.* (2021) 'Biochar in climate change mitigation', *Nature Geoscience*. Springer US, 14(12), pp. 883–892. doi: 10.1038/s41561-021-00852-8.
- Li, C., Zhu, X. and Angelidaki, I. (2020) 'Carbon monoxide conversion and syngas biomethanation mediated by different microbial consortia', *Bioresour. Technol.* Elsevier, 314(May), p. 123739. doi: 10.1016/j.biortech.2020.123739.
- Luo, G. and Angelidaki, I. (2012) 'Integrated biogas upgrading and hydrogen utilization in an anaerobic reactor containing enriched hydrogenotrophic methanogenic culture', *Biotechnology and Bioengineering*. John Wiley & Sons, Ltd, 109(11), pp. 2729–2736. doi: 10.1002/bit.24557.
- Luo, G., Wang, W. and Angelidaki, I. (2013) 'Anaerobic digestion for simultaneous sewage sludge treatment and CO biomethanation: Process performance and microbial ecology', *Environmental Science and Technology*. American Chemical Society, 47(18), pp. 10685–10693. doi: 10.1021/es401018d.
- OECD (1992) *Annex IV - Calculation and Determination of Suitable Summary Parameters, OECD Guideline for Testing of Chemicals*. OECD. Available at: <https://www.oecd.org/chemicalsafety/risk-assessment/1948209.pdf> (Accessed: 3 January 2022).
- Randby, Å. T., Nørgaard, P. and Weisbjerg, M. R. (2010) 'Effect of increasing plant maturity in timothy-dominated grass silage on the performance of growing/finishing Norwegian Red bulls', *Grass and Forage Science*, 65, pp. 273–286. doi: 10.1111/j.1365-2494.2010.00745.x.
- Raya, D. *et al.* (2021) 'Anaerobic Digestion of Aqueous Pyrolysis Liquid in ADM1', *Linköping Electronic Conference Proceedings*, 185, pp. 458–464. doi: 10.3384/ecp21185458.
- Raya, D. (2021) *Analysing Aqueous Pyrolysis Liquid as feed for Anaerobic Digestion*. University of South-Eastern Norway. Available at: <https://openarchive.usn.no/usn-xmlui/handle/11250/2766578> (Accessed: 30 May 2022).
- Seyedi, S. (2020) *Overcoming Anaerobic Digestion Toxicity of Aqueous Liquid from Wastewater Solids Pyrolysis*. Marquette University. Available at: [https://epublications.marquette.edu/dissertations\\_mu/1025](https://epublications.marquette.edu/dissertations_mu/1025) (Accessed: 3 February 2022).
- Seyedi, S., Venkiteswaran, K. and Zitomer, D. (2019) 'Toxicity of various pyrolysis liquids from biosolids on methane production yield', *Frontiers in Energy Research*. Frontiers Media S.A., 7(FEB), pp. 1–12. doi: 10.3389/fenrg.2019.00005.
- Seyedi, S., Venkiteswaran, K. and Zitomer, D. (2020) 'Current status of biomethane production using aqueous liquid from pyrolysis and hydrothermal liquefaction of sewage sludge and similar biomass', *Reviews in Environmental Science and Biotechnology*. Springer Science and Business Media B.V., pp. 237–255. doi: 10.1007/s11157-020-09560-y.
- Shah, S., Bergland, W. H. and Bakke, R. (2017) 'Methane from Syngas by Anaerobic Digestion', *Proceedings of the 58th Conference on Simulation and Modelling (SIMS 58) Reykjavik, Iceland, September 25th – 27th, 2017*. Linköping University Electronic Press, 138, pp. 114–120. doi: 10.3384/ECP17138114.
- Sun, H. *et al.* (2021) 'Modification and extension of an anaerobic digestion model No.1 (ADM1) for syngas biomethanation simulation: From lab-scale to pilot-scale', *Chemical Engineering Journal*. Elsevier B.V., 403, p. 126177. doi: 10.1016/j.cej.2020.126177.
- Torri, C. *et al.* (2020) 'Evaluation of the potential performance of hyphenated pyrolysis-anaerobic digestion (Py-AD) process for carbon negative fuels from woody biomass', *Renewable Energy*. Elsevier Ltd, 148, pp. 1190–1199. doi: 10.1016/j.renene.2019.10.025.
- VDI 4630 (2016) *VDI 4630 - Fermentation of organic materials - Characterization of the substrate, sampling, collection of material data, fermentation tests*, Verein Deutscher Ingenieure e.V. Available at: <https://www.vdi.de/richtlinien/details/vdi-4630-fermentation-of-organic-materials-characterization-of-the-substrate-sampling-collection-of-material-data-fermentation-tests> (Accessed: 30 May 2022).
- Wang, X., Sheng, L. and Yang, X. (2017) 'Pyrolysis characteristics and pathways of protein, lipid and carbohydrate isolated from microalgae *Nannochloropsis* sp.', *Bioresour. Technol.* Elsevier, 229, pp. 119–125. doi: 10.1016/J.BIORTECH.2017.01.018.